# Allosteric inhibition of human ribonucleotide reductase by dATP entails the stabilization of a hexamer

*Nozomi Ando*[a,b,e,‡,*], *Haoran Li*[b,‡], *Edward J. Brignole*[a,b], *Samuel Thompson*[b], *Martin I. McLaughlin*[b], *Julia E. Page*[b], *Francisco J. Asturias*[d], *JoAnne Stubbe*[b,c], *and Catherine L. Drennan*[a,b,c,*]

[a]Howard Hughes Medical Institute, [b]Department of Chemistry, and [c]Department of Biology, Massachusetts Institute of Technology, Cambridge, MA 02139, USA.

[d]Department of Integrative Structural and Computational Biology, The Scripps Research Institute, La Jolla, CA 92037, USA.

[e]Present Address: Department of Chemistry, Princeton University, Princeton, NJ 08544.

‡ These authors contributed equally to this work.

* To whom correspondence should be addressed.

Phone: 609-258-6513 E-mail: nozomi.ando@princeton.edu

Phone: 617-253-5622 E-mail: cdrennan@mit.edu

## SUPPLEMENTAL METHODS

### Expression and Purification of human RNR

*E. coli* BL21(DE3) (Stratagene) was transformed with pET28a-α or pET28a-β and plated on LB agar plates with 50 μg/mL kanamycin, and a single colony was chosen for growth. An overnight culture (60 mL) was diluted into 6 L of LB containing 50 μg/mL kanamycin and grown at 37°C, 250 rpm to an $OD_{600nm}$ of 0.6~0.8. Isopropyl-1-thio-β-d-galactopyranoside (IPTG) was then added to a final concentration of 1 mM, and the cells were grown overnight at 30°C, 250 rpm. The cells were harvested and suspended in 120 mL of **Lysis Buffer** (50 mM $NaH_2PO_4$, pH 7.0, 0.1% Triton X-100, 300 mM NaCl, 10 mM imidazole, and 5 mM 2-mercaptoethanol (BME)) containing 12 tablets of Roche protease inhibitor (Complete, Mini, EDTA-free). The suspension was passed through the French press (2 rounds) at 14,000 psi, followed by centrifugation at 25,000 × *g* for 30 min. The supernatant was treated with streptomycin sulfate to a final concentration of 2% (w/v), and the pellet was removed by centrifugation at 25,000 × *g* for 30 min. The supernatant was treated with 60% $(NH_4)_2SO_4$ (if α was being purified) or 40% $(NH_4)_2SO_4$ (if β was being purified) for 45 min and was subsequently centrifuged at 25,000 × *g* for 30 min. The pellet was then resuspended in 120 mL **Lysis Buffer** and incubated with 12 mL of TALON™ resin (Clontech Laboratories, Inc.) at 4°C for 1 h, which was then loaded into an empty 20-mL column. The column was subsequently washed with 120 mL of 50 mM $NaH_2PO_4$, pH 7.0, 300 mM NaCl, 10 mM imidazole, and 5 mM BME. The protein was then washed with 120 mL of 50 mM $NaH_2PO_4$, pH 7.0, 300 mM NaCl, 5 mM BME, 30 mM imidazole (if α was being purified) or 60 mM imidazole (if β was being purified). α or β was eventually eluted with 120 mL of 50 mM $NaH_2PO_4$, pH 7.0, 300 mM NaCl, 5 mM BME, and 125 mM imidazole. α or β fractions were once more treated with 60% $(NH_4)_2SO_4$ (for α) or 40% $(NH_4)_2SO_4$ (for β) for 45 min and centrifuged at 30,000 × *g* for 30 min. After the supernatant was removed, the pellet was

further condensed by continuing spinning at 30,000 × *g* for 10 min. The remaining supernatant was removed, and the pellet was redissolved in 1~2 mL **Storage Buffer** (For α: 50 mM Tris, 100 mM KCl, 15 mM $MgCl_2$, 5 mM DTT, pH 7.6, 5% glycerol; For β: 50 mM Tris-HCl, pH 7.6, 100 mM KCl, 5% glycerol). Finally, the residual imidazole was removed by a 50-mL Sephadex G-25 column pre-equilibrated with **Storage Buffer**. An activity assay was carried out immediately for α, while β required reconstitution to gain holo-$\beta_2$.[1] Typically, as-purified α has a specific activity of 600~850 nmol dCDP/min/mg. For the following biochemical and biophysical studies, an additional buffer exchange step with Sephadex G-25 chromatography was performed to produce matched buffer solutions. In particular, for SAXS measurements, stock solutions of as-purified ($His_6$-tagged) α were stored in 50 mM HEPES, pH 7.6, 15 mM $MgCl_2$, 5% glycerol, 5 mM DTT.

**Cleavage of N-terminal $His_6$-tag from α**

The N-terminal $His_6$-tag was removed from α by thrombin digestion. As-purified α in **α Storage Buffer** was mixed with thrombin from bovine plasma (Novagen) at a ratio of 2 U (or ~2 $\mu$g) thrombin per 1 mg α. Following incubation at 4 °C for 6~8 h, a 40× solution of Roche protease inhibitor (Complete, Mini, EDTA-free) was added to reach the final working concentration (1×). SDS-PAGE was carried out to confirm the completion of thrombin digestion. Sephadex G-25 chromatography was carried out to prepare stocks solutions of un-tagged α in 50 mM HEPES, pH 7.6, 15 mM $MgCl_2$, 5% glycerol, 5 mM DTT, 150 mM KCl. Un-tagged α prepared for SAXS studies had a specific activity of 861 nmole/min/mg α.

**Reconstitution of β**

Stock solutions of β were deoxygenated by three cycles of evacuation (for 3 × 10 s) followed by Argon flushing (10 min) on a Schlenk line. The deoxygenated β solution and

$Fe(NH_4)_2(SO_4)_2$ (FAS) powder was brought into the Glovebox (MBraun, Stratham, NH). After quantification, FAS stock was added one drop at a time into β solution to reach a final concentration of 5 eq of Fe(II) per $\beta_2$. The reaction was kept stirring at 4°C inside the glovebox for 15 min; meanwhile, $O_2$-saturated **Reconstitution Buffer** (50 mM Tris-HCl, pH 7.6, 100 mM KCl, 5% glycerol) was generated by bubbling pure $O_2$ into the buffer for 15~20 min at 4 °C. After incubation, the protein was removed from the glovebox, and $O_2$-saturated **Reconstitution Buffer** was added to reach 10 eq of $O_2$ per $\beta_2$, followed by blowing $O_2$(g) over the surface of the protein solution for 2 min. The reaction mixture was spun down at 20,000 × g for 5 min to remove the precipitate, and subsequently, Sephadex G-25 chromatography pre-equilibrated with **β Storage Buffer** was carried out to remove excess iron. Holo-$\beta_2$ fractions were collected and saved in small aliquots (100 μL each) for future use. An activity assay was carried out immediately; meanwhile, 250 $\mu$L of the protein solution was placed in an EPR tube and frozen in liquid $N_2$ for measurement of the Y•. Typically, 1~1.2 Y•/β2 were observed with a specific activity of 2000~2400 nmol dCDP/min/mg. For SAXS measurements, an extra Sephadex G-25 chromatography step was performed to store $His_6$-tagged β in 50 mM HEPES, pH 7.6, 15 mM $MgCl_2$, 5% glycerol.

**Expression and Purification of human Trx1**

pET3a-hTrx1 plasmid was obtained from Dr. William Montfort at University of Arizona[2] and transformed into BL21(DE3)pLysS competent cells (Stratagene), and the cells grown on LB agar plate with 100 μg/mL ampicillin at 37 °C. One single colony was picked to inoculate 30 mL LB media with 100 μg/mL ampicillin, and overnight culturing was done at 37 °C, 250 rpm. Subsequently, the overnight culture was used to inoculate 3 L fresh LB media containing 100 μg/mL ampicillin and the cells were grown at 37 °C, 250 rpm until $OD_{600nm}$ = 0.6~0.7. IPTG was added to a final concentration of 1 mM, and the cells were grown at 30 °C,

250 rpm for 16~18 h. Induced cells were harvested at 3,500 × g for 10 min and resuspended into 60 mL of **Lysis Buffer** (50mM Tris-HCl, pH 8.0, 1 mM EDTA, 1 mM PMSF, 5 mM DTT). The cell suspension was then passed through a French press at 14,000 psi for two cycles and spun down at 25,000 × g for 30 min to remove the cell debris. The supernatant was then treated with 2% streptomycin sulfate (w/v), stirred at 4 °C for 10 min and centrifuged at 25,000 × g for 30 min. The supernatant was added to 60 mL of **Q Sepharose Equilibration Buffer** (50 mM Tris-HCl, pH 8.0, 1 mM EDTA, 5 mM DTT) and loaded onto a 30-mL Q Sepharose FF column pre-equilibrated with 150 mL of **Q Sepharose Equilibration Buffer**. The column was first washed with 150 mL of **Q Sepharose Equilibration Buffer,** and the bound proteins were then eluted with a linear gradient from 0 mM to 500 mM NaCl, using 300 mL of **Q Sepharose Equilibration Buffer** and 300 mL of **Elution Buffer** (50 mM Tris-HCl, pH 8.0, 1 mM EDTA, 5 mM DTT, 500 mM NaCl). hTrx1-containing fractions, identified by SDS-PAGE, were pooled, treated with $(NH_4)_2SO_4$ powder to reach 90% (w/v) final concentration, and incubated at 4 °C overnight to complete hTrx1 precipitation. After centrifugation at 25,000 × g, 4 °C for 30 min, the pellet was dissolved in 50 mL of **Sephacryl 26/60 S-200 Equilibration Buffer** (50 mM Tris-HCl, pH 8.0, 1 mM EDTA, 5 mM DTT, 200 mM NaCl), which was further concentrated to around 2 mL using a 3 kDa cut-off Amicon cell (Millipore). The concentrated sample was filtered with a 0.45-μm membrane and then loaded onto a Sepharcryl 26/60 S-200 column (GE Healthcare) pre-equilibrated and washed with **Sephacryl 26/60 S-200 Equilibration Buffer**. The fractions containing hTrx1, identified by SDS-PAGE, were collected and concentrated to <5 mL using a 3 kDa cut-off Amicon cell (Millipore). Finally, DTT and EDTA in hTrx1 were removed using a 50-mL Sephadex G-25 column pre-equilibrated with **Storage Buffer** (50 mM Tris-HCl, pH 8.0, 200 mM NaCl, 5% glycerol). hTrx1-containing fractions, as identified by SDS-PAGE, were pooled and concentrated for future use.

In order to avoid the potential complexities caused by the oxidation of structural cysteines, as-purified hTrx1 was treated with 50-fold excess of DTT at 37 °C for 15 min, and a 50-mL Sephadex G-25 column was used to exchange the protein buffer into 50 mM Tris-HCl, pH 8.0, 1 mM EDTA. Fractions containing hTrx1 were collected, concentrated and saved in small aliquots (50 μL each) for future use. This reduction procedure is modified from a previously published method.[3]

**Expression and Purification of human TrxR1**

Both pET28a-hTrxR1 and pSUABC plasmids were requested from Dr. Vadim N. Gladyshev at Brigham and Women's Hospital and Harvard Medical School.[4] pET28a-hTrxR1 and pSUABC were co-transformed into BL21(DE3) competent cells (Stratagene), and the cells were grown on LB agar plate with 50 μg/mL kanamycin (Km) and 34 μg/mL chloramphenicol (Cm) at 37°C, 250 rpm overnight. One single colony was picked to inoculate 30 mL of LB media with 50 μg/mL Km and 34 μg/mL Cm followed by growth at 37 °C, 250 rpm overnight. The overnight culture was then used to inoculate 3 L of fresh LB media containing 50 μg/mL Km and 34 μg/mL Cm, and the cells were grown at 37 °C until $OD_{600nm}$ = 1.2~1.3. Meanwhile, $Na_2SeO_3$ of 5 μM was added to ensure sufficient selenium supply and suppress Trp incorporation at the UGA,[5] while 100 μg/mL L-Cys was also added to prevent non-specific incorporation of selenium into protein through sulfur pathways.[6] The temperature was then shifted to 30 °C for 1 h with the final $OD_{600nm}$~1.4, and 0.5 mM of IPTG was added to start the induction at 30 °C for 16~18 h. Induced cells of 3 L were harvested at 3,500 × g for 10 min and resuspended into 60 mL of **Lysis Buffer** (50 mM $Na_2HPO_4/NaH_2PO_4$, pH 7.0, 300 mM NaCl, 5 mM BME, Roche complete protease inhibitor tablets). The cell suspension was then passed through the French press cell at 14,000 psi for two cycles and centrifuged at 25,000 × g for 30 min to remove the cell debris. The

supernatant was then treated with 2% streptomycin sulfate, stirred at 4 °C for 10 min, and spun down at 25,000 × g for 30 min. The supernatant was mixed with 10 mL TALON™ affinity resin (Clontech Laboratories, Inc.) pre-washed with 50 mL of **Equilibration Buffer** (50 mM $Na_2HPO_4/NaH_2PO_4$, pH 7.0, 300 mM NaCl, 5 mM BME), followed by gentle shaking on a rocking board at 4 °C for 30 min. The sample-resin mixture was packed into a 10-mL column. The loaded column was first washed with 100 mL of **Equilibration Buffer** and then with 100 mL of **Wash Buffer** (50 mM $Na_2HPO_4/NaH_2PO_4$, pH 7.0, 300 mM NaCl, 5 mM BME, 20 mM imidazole). Finally, hTrxR1 was eluted with 100 mL of **Elution Buffer** (50 mM $Na_2HPO_4/NaH_2PO_4$, pH 7.0, 300 mM NaCl, 5 mM BME, 150 mM imidazole). The BME and imidazole in the hTrxR1 solution were removed with a 50-mL Sephadex G-25 column pre-equilibrated with **Storage Buffer** (50 mM Tris-HCl, pH 7.5, 2 mM EDTA, 5% glycerol). The selenium content in as-purified hTrxR1 was determined by atomic absorption spectroscopy (PerkinElmer) and was used to quantify the concentration of active hTrxR1. Specifically, this hTrxR1 contains 35% Se, which corresponds to 73 μM active hTrxR1.

**hTrx1 and hTrxR1 Activity Assay**

The activities of hTrx1 and hTrxR1 were determined by their ability to reduce insulin disulfides as previously described.[3, 7] 1). For the hTrx1 activity assay: The 500-μL reaction mixture consisted of **TE Buffer** (50 mM Tris-HCl, pH 7.5, 2 mM EDTA), 150 μM NADPH, 160 μM insulin (Sigma), and hTrxR1 dimer (26.5 nM), and hTrx1 (2.5 μM) were added to start the reaction. 2). For the hTrxR1 assay: The 500-μL reaction mixture consisted of **TE Buffer**, 150 μM NADPH, 160 μM insulin (Sigma), and 20 μM hTrx1, and 8.9 nM hTrxR1 dimer were added to start the reaction. For both activity assays, after initiation, the reaction mixture was immediately mixed, and NADPH consumption was monitored by the decrease of $A_{340nm}$, using a sample without addition of hTrx1 (if hTrx1 was being assayed) or hTrxR1

(if hTrxR1 was being assayed) as a control. The turnover numbers for insulin reduction by hTrx1 and hTrxR1 were determined to be 20.5 $min^{-1}$ and 3345.7 $min^{-1}$, respectively.

**Table S1.** Reaction mixtures used to assay α at multiple concentrations.

| | | | | |
|---|---|---|---|---|
| [α] (μM) | 0.5 | 1 | 4 | 10 |
| [β] (μM) | 2.5 | 5 | 20 | 50 |
| [CDP] (mM) | 0.5 | 0.5 | 2 | 5 |
| SA of α (nmol/mg/min) | 722 | 697 | 652 | 642 |
| Turnover ($sec^{-1}$) | 1.11 | 1.07 | 1.00 | 0.99 |

**Table S2.** Data collection and refinement statistics for crystal structure.

| **Data collection** | |
|---|---|
| Beamline | Cornell High Energy Synchrotron Source F1 |
| Space group | $P4_132$ |
| Cell dimensions | |
| $a, b, c$ (Å) | 356.01, 356.01, 356.01 |
| $\alpha, \beta, \gamma$ (°) | 90.0, 90.0, 90.0 |
| Wavelength (Å) | 0.9179 |
| Resolution (Å)† | 75.9 – 9.00 (10.1 – 9.00) |
| Number of unique reflections | 6141 |
| $R_{sym}$ | 0.271 (1.962) |
| $\langle I/\sigma_I \rangle$ | 6.9 (1.7) |
| Completeness (%) | 99.8 (100.0) |
| Redundancy | 15.7 (16.5) |
| **Refinement** | |
| Resolution | 75.9 – 9.00 |
| Number of unique reflections | 6110 |
| $R_{work}/R_{free}$ (%) | 40.54/42.58 |
| B-factor (Å$^2$) | 633.2 |

†Highest resolution shell is shown in parentheses.

**Table S3.** SAXS shape reconstruction statistics for human RNR α subunit in 1 mM CDP in the absence of ATP or dATP (dimeric form) and in the presence of saturating dATP (hexameric form). Experimental scattering profiles were converted into inputs for shape reconstructions in GNOM with "good" Total Estimate scores.[8] The dATP-induced $\alpha_6$ ring was reconstructed in DAMMIN in a cylindrical search space with the outer radius, inner radius, and height specified in parentheses.

| | **α Dimer** | **α Hexamer** |
|---|---|---|
| Data collection parameters | | |
| Beamline | CHESS G1 | CHESS G1 |
| Detector | Pilatus-100K | Pilatus-100K |
| Beam size (defining slits) | 250 μm x 250 μm | 250 μm x 250 μm |
| Energy (keV) | 10.5 | 10.5 |
| Sample-to-detector distance (m) | 1.50 | 1.50 |
| Exposure time | 7 x 5 sec | 2 x 1 sec |
| Concentration (mg $ml^{-1}$) | 0.36 | 0.36 |
| Temperature (K) | 293 | 293 |
| dATP (μM) | 0 | 8 |
| Structural parameters | | |
| $R_g$ (Å) [from Guinier] | 40.6 ± 1.1 | 68.6 ± 2.0 |
| $I(0)$ (a.u.) [from Guinier] | 3.60 ± 0.02 | 11.40 ± 0.16 |
| $D_{max}$ (Å) [from $P(r)$]* | 142.0 | 204.1 |
| $R_g$ (Å) [from $P(r)$]* | 41.4 ± 2.0 | 67.9 ± 0.7 |
| $I(0)$ (a.u.) [from $P(r)$]* | 3.63 ± 0.13 | 11.35 ± 0.15 |
| Porod volume estimate ($Å^3$) | 236550 | 823281 |
| Molecular-mass determination† | | |
| Molecular mass (kDa) from $I(0)$ | 172 | 544 |
| Calculated mass from sequence | 181 | 542 |
| Shape reconstruction statistics | | |
| $q$ range ($Å^{-1}$)* | 0.0152-0.1966 | 0.0149-0.1110 |
| Real space range (Å)* | 0-142.1 | 0-205.0 |
| Shape reconstruction | dammif 1.1.1 | dammin53 |
| Symmetry | P2 | P3 |
| Search space | default | cyl(105,20,110) |
| # Models averaged/total | 9/10 | 10/10 |
| DAMAVER NSD (var) | 0.795 (0.085) | 0.631 (0.027) |

*Refer to Fig. S5C-D. †Determined using 16 μM human β (0.75 mg/mL) as the calibrant.

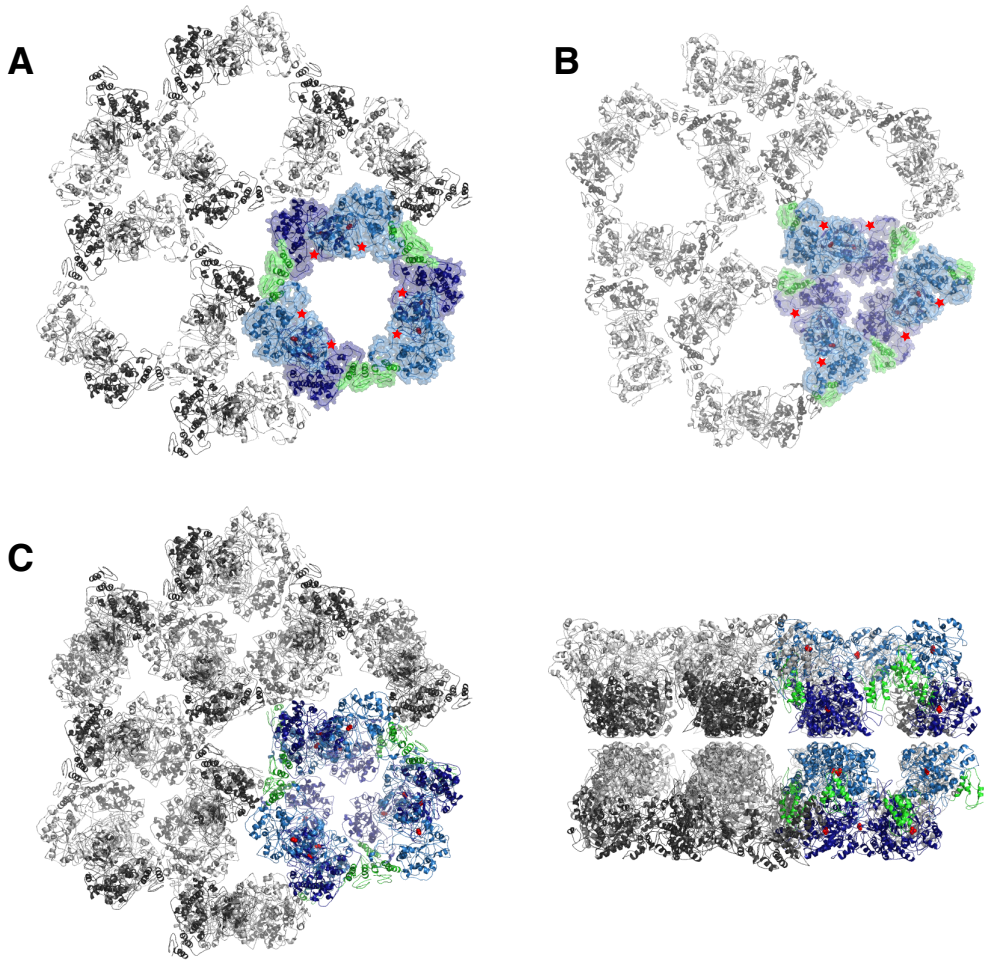


**Figure S1.** Crystal lattice of *Saccharomyces cerevisiae* hexamer co-crystallized with dATP (PDB: 3PAW).[9] (A) For one of the two $\alpha_2$s observed in the asymmetric unit, symmetry-related molecules generate a hexameric ring with the active sites (red stars) pointing inward towards the hole. (B) For the other $\alpha_2$ in the asymmetric unit, symmetry-related molecules generate an inverted hexamer where the active sites (red stars) point outwards. (C) The two hexamers form identical planes (A and B) that are stacked in the crystal lattice.[9] The top and side views of the stacked layers are shown here.

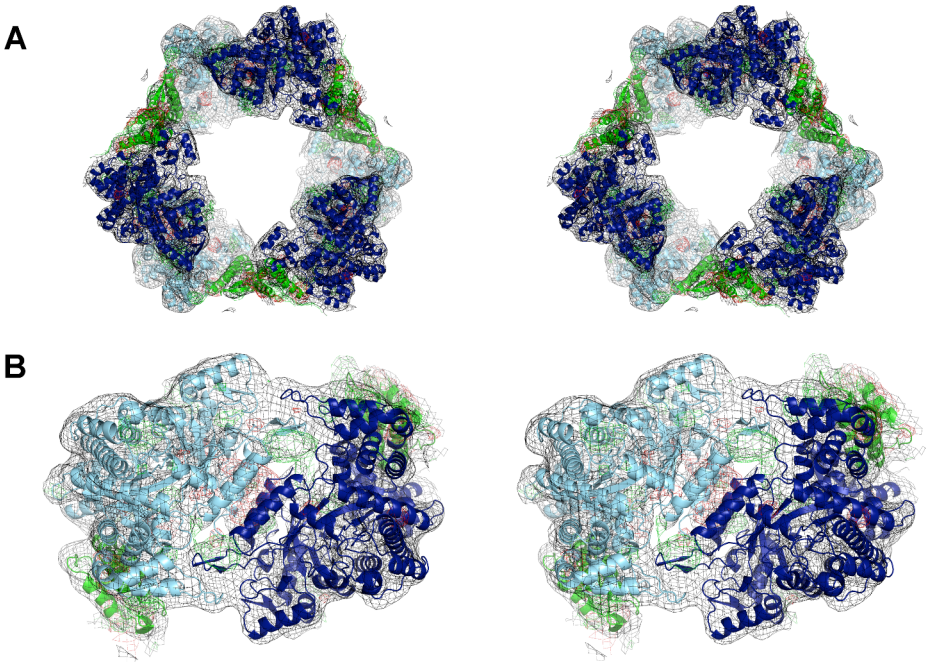


**Figure S2.** Stereoviews of electron density for the crystal structure of human $\alpha_6$ hexamer co-crystallized with dATP at 9-Å resolution shown in Figure 1B of the main text. (A) The hexameric ring, containing three $\alpha_2$ dimers, is generated by crystallographic symmetry. Each asymmetric unit contains one $\alpha_2$ dimer. $2F_o–F_c$ density (black) is contoured at 1.0 σ within 5 Å of atoms; $F_o–F_c$ density (red and green) is contoured at ± 3.0 σ over the same radius. (B) A side view showing the $\alpha_2$ dimer with $2F_o–F_c$ and $F_o–F_c$ density within 5 Å of atoms.

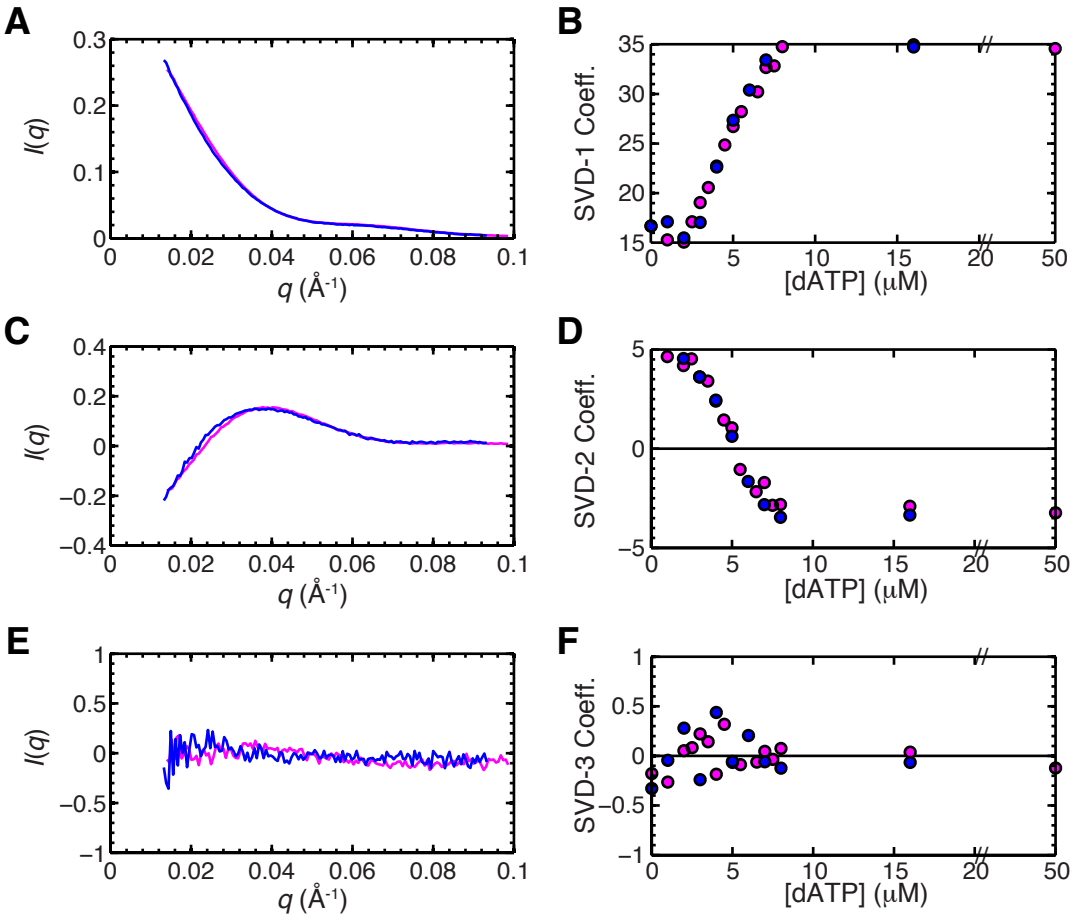


**Figure S3.** Singular value decomposition (SVD) of dATP titration experiments performed on 4 μM α (magenta) and 4 μM $His_6$-tagged α (blue) in the presence of 1 mM CDP. (A) For both constructs, the first singular vector has a meaningful shape, and (B) its associated superposition coefficients display a dATP dependence with a transition midpoint around 4 μM. (C)-(D) Likewise, the second singular vector and its associated superposition coefficients display significant shapes. (E)-(F) In contrast, the third singular vector and its associated superposition coefficients do not display a significant *q*-dependence or dATP-dependence. Both the singular vectors and the coefficients are highly similar with or without the $His_6$-tag. Importantly, these results suggest that the dATP titration data can be described by two states and that the tag has an insignificant effect.

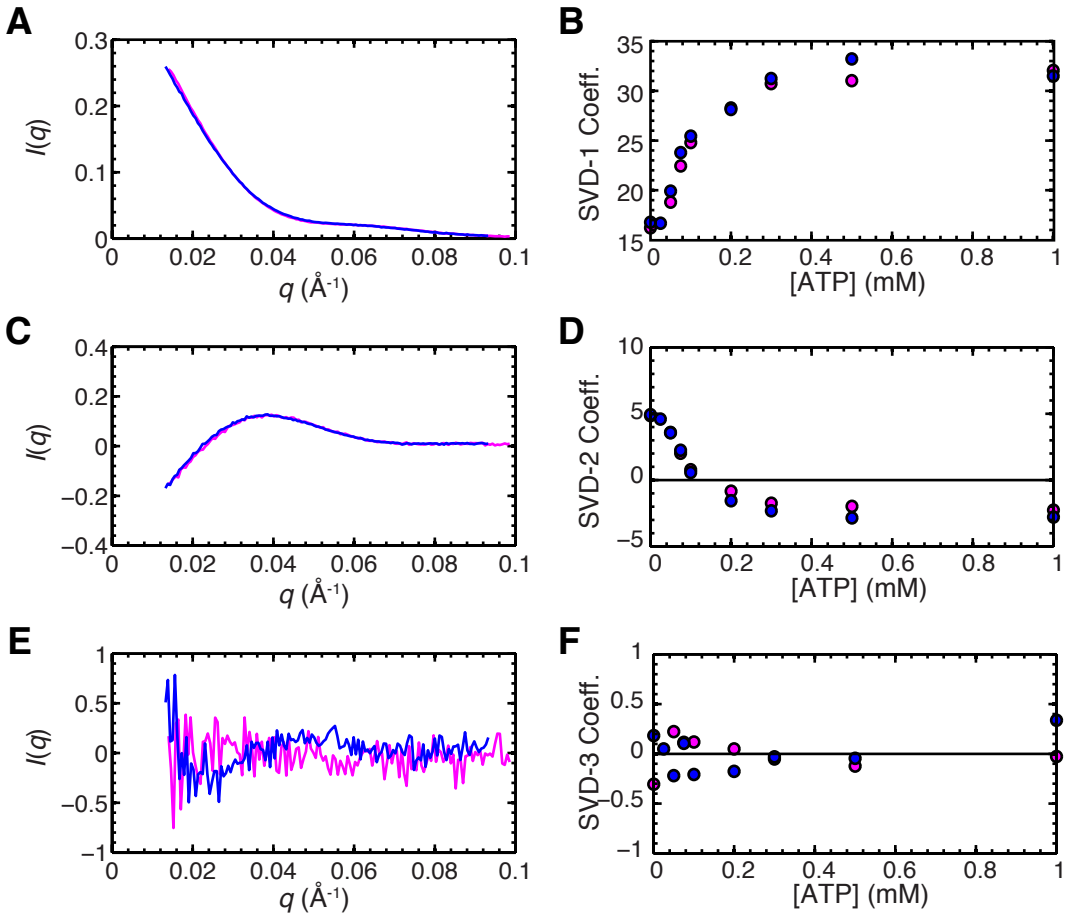


**Figure S4.** Singular value decomposition (SVD) of ATP titration (≤1 mM) experiments performed on 4 μM α (magenta) and 4 μM $His_6$-tagged α (blue) in the presence of 1 mM CDP. (A) For both constructs, the first singular vector has a meaningful shape, and (B) its associated superposition coefficients display an ATP dependence. (C)-(D) Likewise, the second singular vector and its associated superposition coefficients display significant shapes. (E)-(F) For 4 μM α (magenta), the third singular vector and its associated superposition coefficients do not display significant shapes, suggesting that the ATP titration data can be described by two states. In contrast, a slight *q*-dependence can be seen for the $His_6$-tagged α (blue), consistent with the fact that a third state (filaments) can form more readily with the tag. However, the superposition coefficients for the third singular vector are roughly zero in this [ATP] range. In addition, the similarity of the first and second singular vectors and coefficients indicate that the tag has an insignificant effect below 1 mM ATP. Hence, these ATP titration data can be largely described by two states.

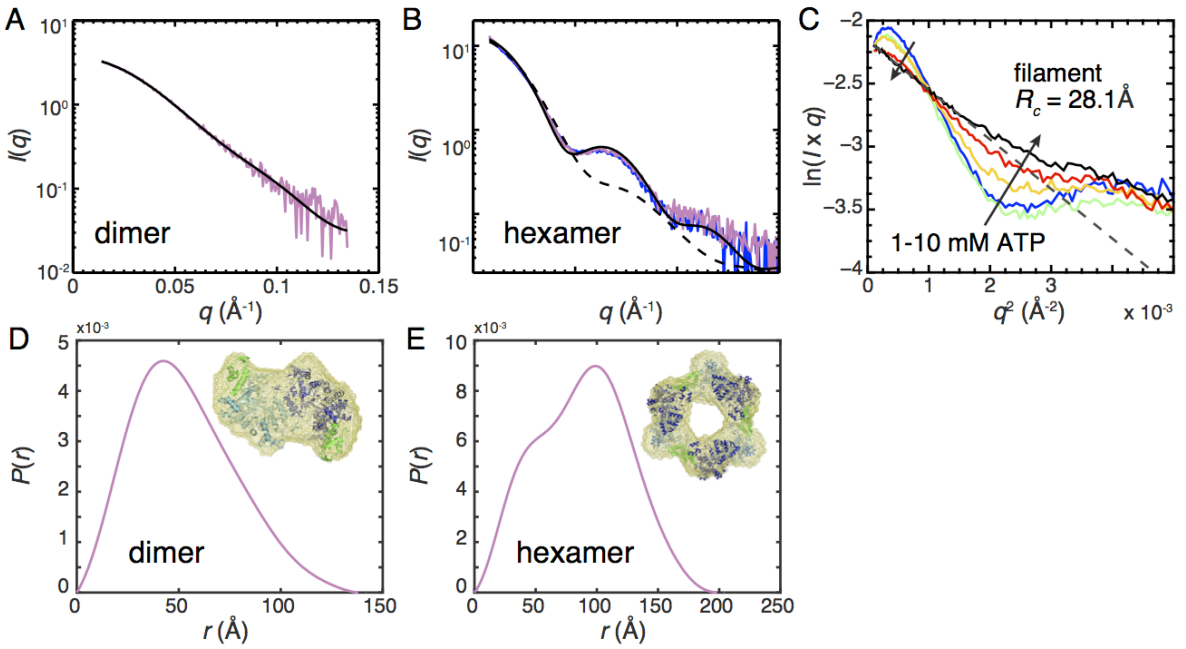


**Figure S5.** SAXS analysis of human α oligomers. All samples contained 1 mM CDP. (A) Scattering from 4 μM α (magenta) is comparable to the theoretical scattering of a previously solved structure of the α dimer (black).[9] (B) Scattering from 4 μM α + 50 μM dATP (magenta) is superimposable with that obtained from 4 μM α + 1 mM ATP (blue). The theoretical scattering of the ring-shaped hexamer (solid black, Supplementary Figure S1A) provides a better fit to both experimental curves ($\chi$ = 0.71-0.86) than the inverted model (dotted black, Supplementary Figure S1B, $\chi$ = 1.88). Here, $\chi$ is defined as the square root of the reduced $\chi^2$.[10] (C) The scattering curves from 4 μM α + 1-10 mM ATP (same coloring as Fig. 3A in the main text) and that of 4 μM $His_6$-tagged α + 10 mM ATP (black) are plotted here as cross-sectional Guinier plots: ln($I$ x $q$) vs $q^2$. The low $q$ region becomes increasingly linear with the addition of ATP, indicating that a highly elongated species with a well-defined $R_c$ is forming. (D) The pair distance distribution function, $P(r)$, of 4 μM α in the absence of effectors shows a skewed shape, as expected for a dimer. (E) $P(r)$ of 4 μM α + 50 μM dATP displays two peaks consistent with a hexamer: one corresponding to the distances within individual subunits and another corresponding to the cross-ring distances.

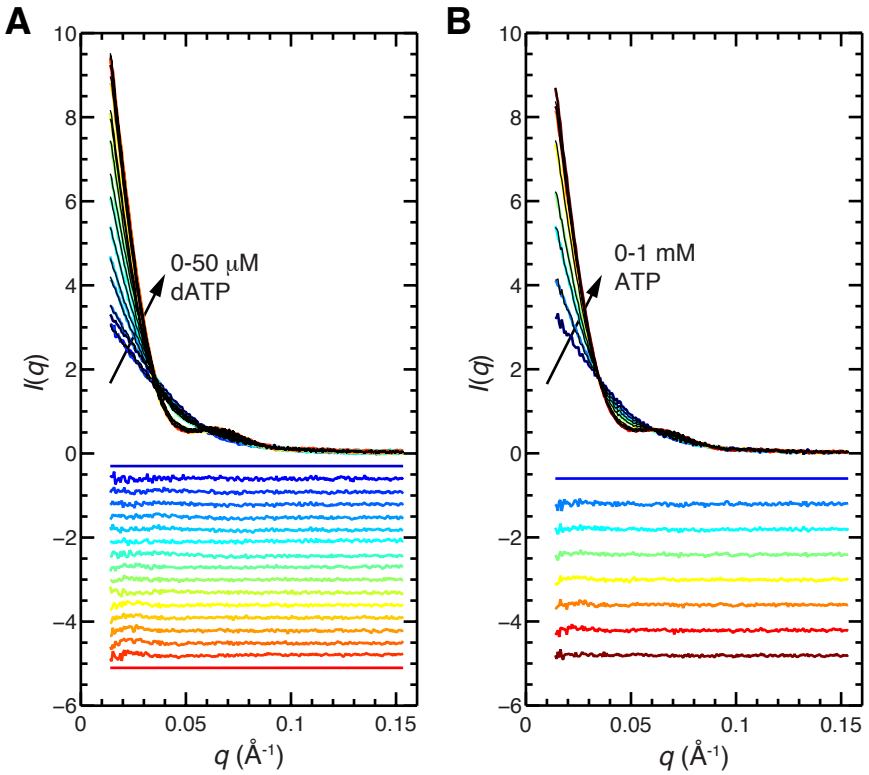


**Figure S6.** Changes in scattering from 4 μM α in the presence of 0-50 μM dATP (Figure 2A) or 0-1 mM ATP (Figure 2D) are consistent with dimer-hexamer transitions for human RNR. (A) Linear combinations of the scattering from 0 μM dATP (representing the dimer) and 50 μM dATP (representing the hexamer) provide good fits (black) to the scattering curves obtained over the course of the dATP titration (blue to red). The residuals from the fits (shown below with constant offsets) are largely flat and featureless. (B) Linear combinations of the same two scattering curves used in (A) also provide good fits (black) to the scattering curves obtained over the course of the ATP titration (blue to red), as indicated by the flat residuals (shown below with constant offsets).

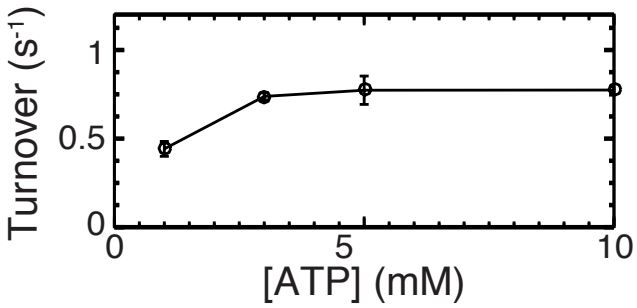


**Figure S7.** Activity of human RNR at high ATP concentrations. Turnover was measured at high ATP in the presence of 4 μM α, a five-fold excess of β, and radioactively labeled substrate (2 mM [5-$^{3}$H]-CDP). Although the protein stocks used for this assay yielded lower turnover numbers than those in Figure 2F in the main text, a similar increase in activity is observed up to 3 mM ATP. Above 3 mM ATP, no significant change in activity is observed.

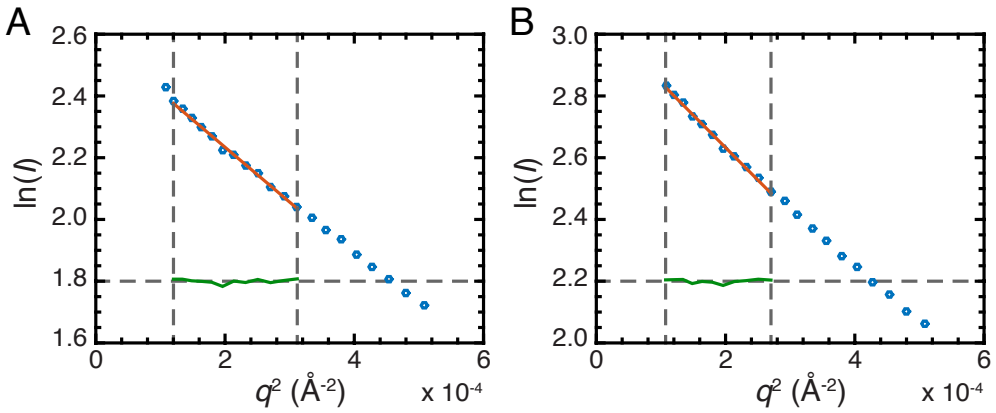


**Figure S8.** Effect of β subunit on the effective radius of gyration ($R_g$) of dATP-treated α. (A) A Guinier plot of the scattering from 4 μM α in 50 μM dATP (black curve in Figure 4) shows linearity at low $q$. A linear fit (red) over the region satisfying the condition $q_{max}R_g$<1.3 yields an $R_g$ value of 72.9 ± 1.7 Å. (B) The Guinier plot of the scattering from 4 μM α + 4 μM β in 50 μM dATP (red curve in Figure 4) also shows linearity and yields an $R_g$ value of 79.3 ± 3.0 Å.

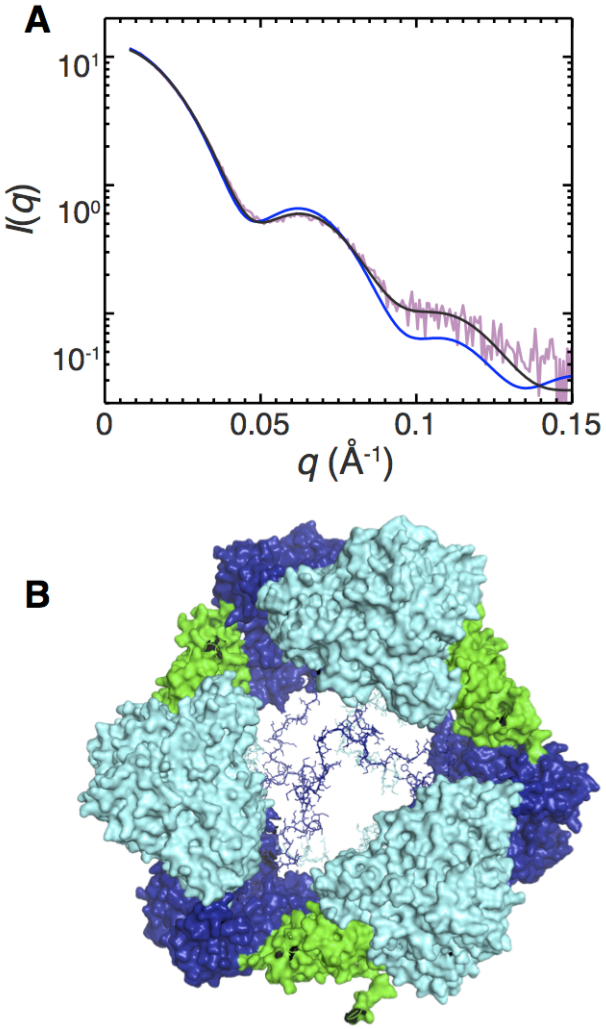


**Figure S9.** Modeling the disordered C-terminal tails (residues 743-792) of α improves fit to SAXS data. The missing residues from the disordered C-termini were modeled into the crystal structure determined in this study with Modeller and constant-temperature molecular dynamics implemented in AllosMod-FoXS.[10, 11] (A) The theoretical scattering of the crystal structure human $\alpha_6$ obtained in this study (blue) provides a reasonable fit ($\chi$ = 0.71) to the SAXS data collected on 4 μM α in 50 μM dATP, 1 mM CDP (pink). Modeling the missing residues improves the fit (black, $\chi$ = 0.45), particularly in the position of the oscillation at ~0.07 Å$^{-1}$. (B) This improved fit is obtained by allowing the C-terminal tails (shown as sticks) to take up space inside the hexameric ring (shown in surface representation). Here, $\chi$ is defined as the square root of the reduced $\chi^2$.[10]

## Supplementary References

[1] Wang, J., Lohman, G. J. S., and Stubbe, J. (2009) Mechanism of inactivation of human ribonucleotide reductase with p53R2 by gemcitabine 5'-diphosphate, *Biochem. 48*, 11612-11621.

[2] Weichsel, A., Gasdaska, J. R., Powis, G., and Montfort, W. R. (1996) Crystal structures of reduced, oxidized, and mutated human thioredoxins: evidence for a regulatory homodimer, *Structure 4*, 735-751.

[3] Ren, X., Björnstedt, M., Shen, B., Ericson, M. L., and Holmgren, A. (1993) Mutagenesis of structural half-cystine residues in human thioredoxin and effects on the regulation of activity by selenodiglutathione, *Biochem. 32*, 9701-9708.

[4] Turanov, A. A., Su, D., and Gladyshev, V. N. (2006) Characterization of alternative cytosolic forms and cellular targets of mouse mitochondrial thioredoxin reductase, *J Biol Chem 281*, 22953-22963.

[5] Liu, Z., Reches, M., and Engelberg-Kulka, H. (1999) A sequence in the *Escherichia coli* fdhF "selenocysteine insertion Sequence" (SECIS) operates in the absence of selenium, *J Mol Biol 294*, 1073-1086.

[6] Muller, S., Heider, J., and Bock, A. (1997) The path of unspecific incorporation of selenium in *Escherichia coli*, *Arch Microbiol 168*, 421-427.

[7] Arnér, E. S., and Holmgren, A. (2001) Measurement of thioredoxin and thioredoxin reductase, *Curr Protoc Toxicol Chapter 7*, Unit 7.4.

[8] Svergun, D. I. (1992) Determination of the regularization parameter in indirect-transform methods using perceptual criteria, *J. Appl. Crystallogr. 25*, 495-503.

[9] Fairman, J. W., Wijerathna, S. R., Ahmad, M. F., Xu, H., Nakano, R., Jha, S., Prendergast, J., Welin, R. M., Flodin, S., Roos, A., Nordlund, P., Li, Z., Walz, T., and Dealwis, C. G. (2011) Structural basis for allosteric regulation of human ribonucleotide reductase by nucleotide-induced oligomerization, *Nat. Struct. Mol. Biol. 18*, 316-322.

[10] Schneidman-Duhovny, D., Hammel, M., and Sali, A. (2010) FoXS: a web server for rapid computation and fitting of SAXS profiles, *Nucleic Acids Res. 38*, W540-544.

[11] Weinkam, P. P., Pons, J. J., and Sali, A. A. (2012) Structure-based model of allostery predicts coupling between distant sites, *Proc. Natl. Acad. Sci. U. S. A. 109*, 4875-4880.